# Creep anomaly in electrospun fibers made of globular proteins

Omri Regev,[1] Arkadii Arinstein,[2] and Eyal Zussman[1,2,*]

[1]*Russell Berrie Nanotechnology Institute, Technion–Israel Institute of Technology, Haifa 32000, Israel*

[2]*Department of Mechanical Engineering, Technion–Israel Institute of Technology, Haifa 32000, Israel*

(Received 11 October 2012; revised manuscript received 21 October 2013; published 30 December 2013)

The anomalous responses of electrospun nanofibers and film fabricated of unfolded bovine serum albumin (BSA) under constant stress (creep) is observed. In contrast to typical creep behavior of viscoelastic materials demonstrating (after immediate elastic response) a time-dependent elongation, in case of low applied stresses (<1 MPa) the immediate elastic response of BSA samples is followed by gradual contraction up to 2%. Under higher stresses (2–6 MPa) the contraction phase changes into elongation; and in case of stresses above 7 MPa only elongation was observed, with no initial contraction. The anomalous creep behavior was not observed when the BSA samples were subjected to additional creep cycles independently on the stress level. The above anomaly, which was not observed before either for viscoelastic solids or for polymers, is related to specific protein features, namely, to the ability to fold. We hypothesize that the phenomenon is caused by folding of BSA macromolecules into dry molten globule states, feasible after cross-linked bonds break up, resulting from the applied external force.

DOI: 10.1103/PhysRevE.88.062605 PACS number(s): 36.20.−r, 87.15.La, 62.20.Hg

## I. INTRODUCTION

When an ideal elastic material is subjected to a constant stress, its immediate strain response remains constant. In contrast, viscoelastic polymers undergo creep, a time-dependent viscoplastic response, in which molecular motion (reptation) results in monotonic elongation of the material over time [1–3]. A material's creep response can be dictated by specific structural features (e.g., degree of polymer matrix heterogeneity) and presents a great challenge in engineering applications, where designers try to increase the creep resistance of polymers [4,5] and composite materials [6–9]. In biopolymers [10], biofibers [11], and soft biological tissues [12], creep response may indicate structural and biochemical changes [13].

Herein, we report a creep anomaly observed in structures made of bovine serum albumin (BSA). The BSA was denatured, which involved reduction of disulfide bonds and concomitant controlled protein unfolding, providing for the reformation of new, extended, polymer-like structures rich in strong inter- and intramolecular disulfide bonds [14]. When exposed to tensile stress, the denatured material demonstrated a nonmonotonic creep response, with an initial rapid elastic elongation phase, followed by an unexpected contraction (decreased creep rate), and only thereafter a phase which exhibited creep behavior typical of polymers (gradual increase of creep rate). A similar nonmonotonic time response was reported in creep experiments of ultrahigh-molecular-weight polyethylene [15]; however, unlike the BSA, the contraction was an order of magnitude lower and was instead related to relaxation after intensive preloading.

## II. MATERIALS AND METHODS

Experiments were conducted on BSA fibers electrospun [14,16] from a solution of 10 wt% BSA in 2,2,2-trifluoroethanol (TFE), distilled water, and 2-mercaptoethanol (ME; 0.2 g per 1 g BSA). Aligned fiber mats were collected on a vertical rotating wheel (1500 rpm) [17]. Films of BSA were prepared by solution casting on Teflon dishes. All samples were stored for at least one month in a vacuum of $\sim 10^{-3}$ atm, and then stored at room temperature under ambient conditions for 2 or 18 months after fabrication. A dynamic mechanical analyzer (DMA) was used to test rectangular-shaped samples ($10 \times 5 \times 0.1$ mm$^3$) mounted using a torque-meter (2 lb-in.). Load was applied along the fiber axis of the mat. All tests were conducted at room temperature, in 40–70% relative humidity.

## III. RESULTS

Quasistatic tensile tests (strain rate of 1%/min) showed that fiber mat strength was $13.0 \pm 1.6$ MPa ($n = 12$), with $5.8 \pm 1.2$% extensibility, and an elastic modulus of $514 \pm 121$ MPa (calculated over a strain range of 0.2–0.8%). Figure 1 shows the results of creep experiments conducted under tensile stresses of 1, 4, and 8 MPa. Fiber mats broke up above stresses of ∼9 MPa. At stresses below 5 MPa, fiber mats demonstrated a unique contraction behavior (see Fig. 1). The creep response started with an elastic response that lasted 0.36 s, followed by continuous elongation for 0.5–20 s and gradual contraction over time. At low stresses (<5 MPa) contraction was dominant, while contraction was suppressed by creep elongation when stresses have exceeded 6 MPa.

When a mounted fiber mat was tested in the second cycle the contraction creep phase was absent, while the creep rate slowly increased with time, as expected of polymeric viscoelastic materials (see Fig. 2). This response was observed for all tested stresses between 1 to 8 MPa. The elastic modulus of fiber mats in the second creep cycle was higher in $350 \pm 100$ MPa than that of the first cycle (see the instantaneous response in Fig. 2), a change which proved to be stress independent.

At first glance, the creep anomaly of BSA fiber mats may be attributed to the strong extension of the polymer matrix during the electrospinning process [19] and, possibly, to confinement [20]. However, the unexpected contraction was also observed in films cast from the same BSA solution used for fiber fabrication (see Fig. 3). In both cases, the BSA chains are

*meeyal@technion.ac.il

 ©2013 American Physical Society

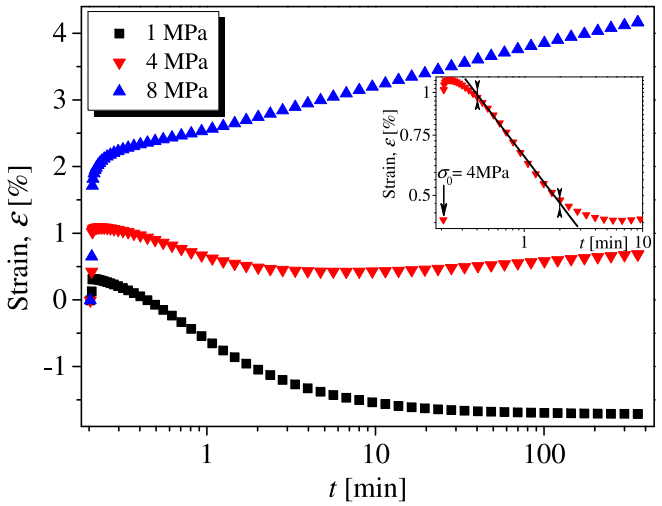


FIG. 1. (Color online) Creep experiments conducted on BSA fibers: strain vs lg(time) responses are plotted for stresses of 1, 4, and 8 MPa applied on electrospun BSA fibers. Strain was monitored for 6 h. The inset shows a log-log scale of strain vs time (4 MPa), and the slopes of the straight lines correspond to the exponents in scaling dependences describing contraction.

unfolded (open) in the protein solution due to good polymer-solvent interactions (TFE) and to reduction of intramolecular disulfide bonds (ME) [21,22]. As intermolecular disulfide bonds reform during solvent evaporation and under subsequent oxidative ambient conditions [14], we hypothesize that chains in the BSA fibers and films become locked in an unfolded state. This hypothesis is supported by frequency sweep tests of BSA fibers, where storage and loss moduli were independent of the applied frequency—typical of a cross-linked network [23]. As a result of external stress some weak bonds can break up, allowing for further changes in the polymer network structure.

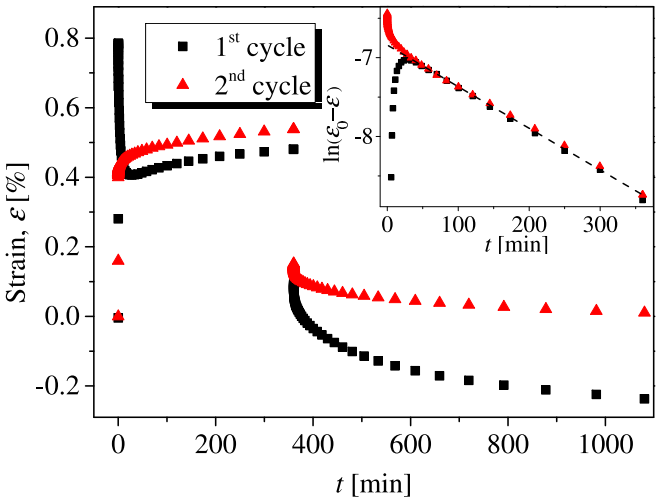


FIG. 2. (Color online) Two sequential creep cycles conducted on BSA fibers. The applied tensile stress was 3 MPa. Note the increase in elastic modulus, as shown by the lower immediate strain response of the second creep cycle. The inset shows the long-term exponential creep in the first and second cycles.

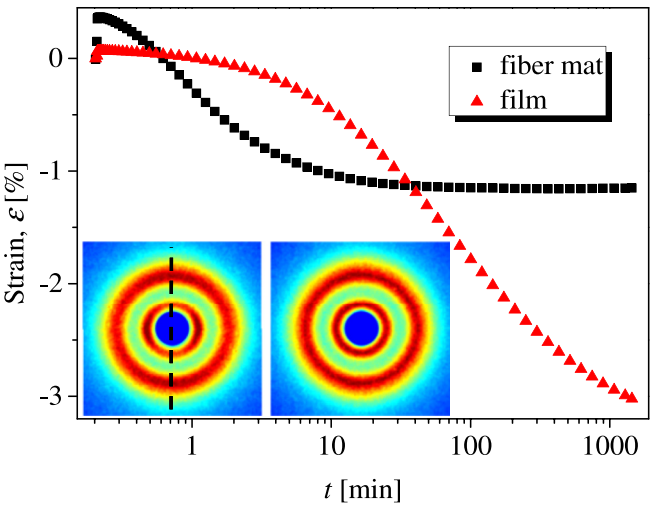


FIG. 3. (Color online) Strain vs log (time) responses of BSA fiber mat and film under an applied tensile stress of 1 MPa. Strain was monitored for 24 h. The inset shows scattering images of a BSA fiber mat (left) and film (right) obtained from wide-angle x-ray scattering (WAXS) measurements. The dashed line shows the fiber's axis in the tested mat. The small $d$ spacing (4.3 Å) is suggested to be related to the backbone distance within the $\alpha$ helixes, while the larger $d$ spacing (9.2 Å) is attributed to lateral $\alpha$-helix segment packing.

In particular, a portion of unfolded BSA chains can relax into dry molten globule states. According to our hypothesis, just this folding of BSA molecules results in the observed contraction of BSA samples. Evolution of a sample structure corresponding to a nonmonotonic response to constant tensile stress is depicted schematically in Fig. 4. This hypothesis can be supported by the model shown below.

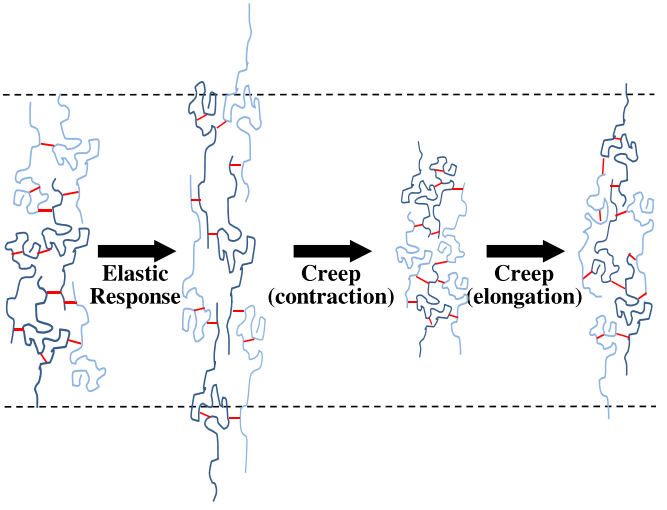


FIG. 4. (Color online) Illustration of the BSA matrix evolution during creep tests. For clarity, BSA chains are designated with two shades of blue (gray); red (gray) lines depict disulfide bonds. (a) BSA matrix of electrospun fibers; (b) the stretched matrix immediately after applying stress and breaking of some disulfide bonds; and (c) the matrix after contraction due to folding of portion of albumin macromolecules under constant load.

TABLE I. Parameters of the material response obtained under various stresses.

| Stress (MPa) | | 1 | 2 | 3 | 4 | 5 | 6 | 7 | 8 |
|---|---|---|---|---|---|---|---|---|---|
| $a$ (%) | | 3.4 | 2.2 | 1.6 | 1.0 | 0.25 | $\ll$0.1 | $\ll$0.1 | $\ll$0.1 |
| $\varepsilon_\infty$ (%) | | $-1.4$ | $-0.4$ | 0.2 | 0.8 | 2.1 | 2.2 | 2.7 | 0.37 |
| Fast | $A_1$ (%) | 0.045 | 0.090 | 0.093 | 0.20 | 0.19 | 0.21 | 0.25 | 0.62 |
| | $\tau_1$ (min) | 46 | 27 | 27.5 | 9.2 | 5.7 | 19.5 | 9.3 | 6.0 |
| Slow | $A_2$ (%) | 0.053 | 0.085 | 0.144 | 0.254 | 0.50 | 0.38 | 0.56 | 0.73 |
| | $\tau_2$ (min) | 95 | 203 | 181 | 106 | 88 | 163 | 120 | 92 |

## IV. MODELING

When an instantaneous tensile load is applied, the BSA network elongates (elastic response), under constraints of topology (entanglement points), and the disulfide bonds (230 kJ/mol), which are weak compared to the backbone C–C (350 kJ/mol) and C–N (300 kJ/mol) bonds, can then break up. These broken disulfide bonds can be restored due to pair interactions. In addition, the BSA chains can then relax into dry molten globule states [24–26], which lower in free energy, triggering contraction of the entire fiber mat. Both these processes result in decrease in free bond amount, but during the initial stage, the impact of the last one into the restore kinetics of free bonds is negligible. Thus, the bond restore can be approximated by a kinetic process of the second order and is described by the following equation:

$$\frac{dc_b(t)}{dt} = -k_b c_b^2(t), \tag{1}$$

which results in a power drop in the number of free bonds, $c_b$:

$$c_b(t) = \frac{c_{b,0}}{1 + t/\tau_b}, \tag{2}$$

where the specific time, $\tau_b$, is $\tau_b = 1/k_b c_{b,0}$, $k_b$ is the constant of the bond restore process, and $c_{b,0}$ is the initial concentration of free bonds.

The rate of the BSA chains relaxation into dry molten globule states is proportional to the number of free bonds

$$\frac{dc_f(t)}{dt} = k_f c_b(t), \tag{3}$$

where $k_f$ is the relaxation constant.

The contraction rate is proportional to folding rate, $dc_f/dt$, as well as to a factor $l(t) - l_{\min}$:

$$\frac{dl(t)}{dt} = -k_l[l(t) - l_{\min}]\frac{dc_f(t)}{dt}, \tag{4}$$

where $k_l$ is the constant of fiber contraction process, $l(t)$ is the current fiber length, and $l_{\min}$ is the fiber length at which the stretching forces oppose the folding possibility.

The solution of Eq. (4) together with Eqs. (2) and (3) results in a scaling law of the strain, $\varepsilon = l(t)/l_0 - 1$ ($l_0$ is the initial unstretched fiber length), describing the fiber contraction:

$$\begin{aligned}\varepsilon_1(t) &= \varepsilon_\infty + (\varepsilon_0 - \varepsilon_\infty)\exp[-k_l c_f(t)] \\ &= \varepsilon_\infty + \frac{a}{(1 + t/\tau_b)^\alpha},\end{aligned} \tag{5}$$

where $a = \varepsilon_0 - \varepsilon_\infty$, $\varepsilon_0$ is initial fiber strain, the final strain $\varepsilon_\infty = l_{\min}/l_0 - 1$, and $\alpha = k_l k_f/k_b$.

Simultaneously, the molecular motion (reptation) causes protein chains to flip and rotate under constraints of reforming S–S cross links, resulting in monotonic elongation. Assuming a quasilinear viscoelastic behavior of the system in question, the relaxation according to an exponential law, $\varepsilon_2(t) = A[1 - \exp(-t/\tau)]$, is expected. However, the measured strain data ($t > 100$ min, stress $> 2$ MPa) cannot be fitted by this exponential function. This fact indicates that the electrospun BSA fibers have a spectrum of relaxation times due to their highly heterogeneous structure. In such a situation the concept of polychromatic kinetics could be applied [27].

A possible widely accepted way to take into account the polychromatic character of the relaxation process is to introduce, in place of spectrum of relaxation times, two characteristic relaxation times, $\tau_1$ and $\tau_2$ ($\tau_1 \gtrsim \tau_{\min}$ and $\tau_2 \lesssim \tau_{\max}$). The shortest characteristic time, $\tau_1$, corresponds to the fast relaxation in a part of the sample, whereas the longest one, $\tau_2$, corresponds to the slow relaxation in remaining (unrelaxed) part of the sample. In this approximation the relaxation process can be described by the following equation:

$$\varepsilon_2(t) = A - A_1\exp(-t/\tau_1) - A_2\exp(-t/\tau_2), \tag{6}$$

where $A = A_1 + A_2$.

The resulting response of the streched fibers can be described as the sum of $\varepsilon_1(t)$ and $\varepsilon_2(t)$, Eqs. (5) and (6), respectively:

$$\varepsilon(t) = \varepsilon_1(t) + \varepsilon_2(t). \tag{7}$$

The analysis of the experimental data was carried out in two steps. At first (for stresses $< 6$ MPa, when the contraction was observed), the shortening of the samples was fitted by Eq. (5). Fitting strain data with a power law (5), we find that the parameters $\alpha$ and $\tau_b$ demonstrate only small fluctuation with the applied stress. At the second step, the full response (both contraction and creep) of the samples for all applied stresses was fitted by Eq. (7) ($R^2 > 0.99$), using the average values of $\alpha = 0.75$ and $\tau_b = 16.47$ s. In such a way the parameters $a$, $\varepsilon_\infty$, $A_1$, $A_2$, $\tau_1$, and $\tau_2$ were found (see Table I). Typical fittings of experimental data for applied stresses of 2, 3, and 7 MPa are presented in Fig. 5.

## V. DISCUSSION AND CONCLUSIONS

The obtaind results show that when increasing the tensile stress, the amplitude, $a$, decreases whereas the final strain, $\varepsilon_\infty$, increases from negative to positive strain, since the elongation, caused be external forces, is more dominant than the contraction due to internal stresses. As expected, both

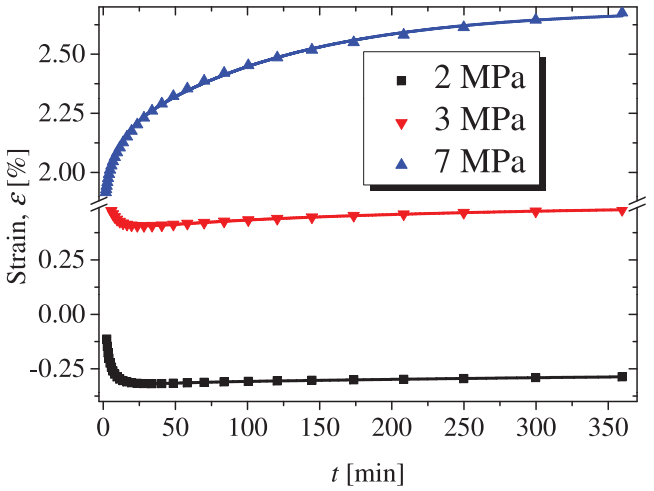


FIG. 5. (Color online) Typical fitting of experimental data for applied stresses: 2, 3, and 7 MPa. (i) 2 MPa: $a = 1.65\%, \varepsilon_\infty = -0.27\%, A_1 = 7.7 \times 10^{-2}\%, \tau_1 = 30$ min, $A_2 = 7.4 \times 10^{-2}\%, \tau_2 = 309$ min; (ii) 3 MPa: $a = 1.49\%$, $\varepsilon_\infty = 0.5\%$, $A_1 = 6.2 \times 10^{-2}\%$, $\tau_1 = 27$ min, $A_2 = 0.12\%$, $\tau_2 = 230$ min; and (iii) 7 MPa: $a \ll 0.01\%$, $\varepsilon_\infty = 2.7\%, A_1 = 0.25\%, \tau_1 = 9.3$ min, $A_2 = 0.56\%, \tau_2 = 119$ min. In all cases $R^2 > 0.999$.

creep amplitudes $A_1$ and $A_2$, corresponding to fast and slow relaxations, respectively, are increasing proportional to the tensile stress, whereas their ratio, $A_1/A_2$, is decreasing. The fast characteristic relaxation time, $\tau_1$, decreases inversely to tensile stress, saturating at high stresses, whereas the slow characteristic relaxation time, $\tau_2$, demonstrates irregular variations (the irregularity at 6 MPa is, apparently, due to fluctuations). Such type of behavior is reasonable: The fast characteristic relaxation time, $\tau_1$, is related to the probability of overcoming the regular energy barrier, whereas the slow characteristic relaxation time, $\tau_2$, is related to a heterogeneity (imperfections) of polymer matrix and thus is only weakly dependent on the tensile stress.

The strain data, obtained in the second creep cycle, also demonstrates a polychromatic kinetics [27], as in the first creep cycle. One can fit the strain data of the second creep cycle by power function, $\sim t^\nu$, with $\nu \sim 0.3$, that is similar to the exponents previously measured for biopolymers [5] and synthetic polymers [18]. Nevertheless, in order to compare the creep kinetics in the first and the second cycles, it is quite reasonable to describe the strain data, obtained in the second cycle, also with the help of Eq. (6). It turned out that the initial creep rate in the second cycle significantly increases compared to the first cycle ($\tau_1 \sim 10^2$ s), while the long-time asymptotes ($t > 100$ min) result in a similar creep rate ($\tau_2 \sim 10^4$ s) for both first and second creep cycles (see inset in Fig. 2).

Note that along with strongly interconnected skeleton a random polymer network contains also dangling tails weakly connected with network. Only these BSA tails can change their state, relaxing into dry molten globule states, whereas no folding of strongly interconnected macromolecules is observed. Such point of view allows one to explain the nonmonotonic sample response, when after prolonged exposure, even under low stresses, the contraction stops, giving place to elongation. Similarly, in the second creep cycle, chain unfolding no longer occurs, and thus samples creep as expected under both low and high stress. Samples subjected to low stress (1 MPa) as well as to high stress (>7 MPa) in the first creep cycle, followed by a second creep cycle under low stress (1 MPa), creep regularly throughout the second cycle (see Fig. 2).

It is worth noting that BSA films contract even when subjected to tensile stresses (e.g., 20 MPa) close to their ultimate tensile strength value of ~25 MPa (as determined in quasistatic tests). The film contraction rate is slower, but eventually more evident, than fiber mat contraction (see Fig. 3). These differences are attributed to the fact that BSA fibers show molecular orientation, wherein intra-$\alpha$-helix distances (~4.3 Å) [14,28] are ordered along the fiber axis, while the inter-$\alpha$-helix distances (~9.2 Å) tend to orientate perpendicular to the fiber axis (see inset in the Fig. 3). In contrast, the cast film is isotropic.

The change in modulus following high stress application is attributed to enhanced crystal alignment during the creep phase [29,30]. Under low stresses, it is assumed that increase in the density of cross links can explain the enhanced modulus.

In conclusion, this work explored the creep anomaly of BSA fibers and films, in which the contraction phase is attributed to macromolecules folding. Successive creep cycles yielded creep responses typical of polymers.

## ACKNOWLEDGMENTS

We acknowledge the financial support of the Russell Berrie Nanotechnology Institute (RBNI) at the Technion and the Israel Sceince Foundation (ISF, Grant No. 770/11). A.A. acknowledge the financial support of Kamea Program of the Israel Ministry of Absorption.

[1] J. D. Ferry, *Viscoelastic Properties of Polymers* (Wiley, New York, 1980).
[2] J. J. M. Baltussen and M. G. Northolt, Polymer **42**, 3835 (2001).
[3] M. Siebenburger, M. Ballauff, and T. Voigtmann, Phys. Rev. Lett. **108**, 255701 (2012).
[4] T. Higashioji and B. Bhushan, J. Appl. Polym. Sci. **84**, 1477 (2002).
[5] J. F. Martucci, R. A. Ruseckaite, and A. Vazquez, Mater. Sci. Eng., A **435**, 681 (2006).
[6] Z. Zhang, J. L. Yang, and K. Friedrich, Polymer **45**, 3481 (2004).
[7] H. Nechad, A. Helmstetter, R. El Guerjouma, and D. Sornette, Phys. Rev. Lett. **94**, 045501 (2005).
[8] T. H. Zhou, W. H. Ruan, J. L. Yang, M. Z. Rong, M. Q. Zhang, and Z. Zhang, Compos. Sci. Technol. **67**, 2297 (2007).
[9] J. Yang, Z. Zhang, K. Friedrich, and A. K. Schlarb, Macromol. Rapid Commun. **28**, 955 (2007).

[10] Y. Yang, J. Lin, B. Kaytanli, O. A. Saleh, and M. T. Valentine, Soft Matter **8**, 1776 (2012).
[11] C. Smith, J. Ritchie, F. I. Bell, I. J. McEwen, and C. Viney, J. Arachnol. **31**, 421 (2003).
[12] Y. C. Fung, *Biomechanics: Mechanical Properties of Living Tissues* (Springer-Verlag, Berlin, 1993).
[13] W. R. Trickey, G. M. Lee, and F. Guilak, J. Orthop. Res. **18**, 891 (2000).
[14] Y. Dror, T. Ziv, V. Makarov, H. Wolf, A. Admon, and E. Zussman, Biomacromolecules **9**, 2749 (2008).
[15] F. Khan and C. Yeakle, Int. J. Plast. **27**, 512 (2011).
[16] O. Regev, S. Vandebril, E. Zussman, and C. Clasen, Polymer **51**, 2611 (2010).
[17] S. A. Theron, E. Zussman, and A. L. Yarin, Nanotechnology **12**, 384 (2001).
[18] H. Liu, M. A. Polak, and A. Penlidis, Polym. Eng. Sci. **48**, 159 (2008).
[19] A. Arinstein and E. Zussman, J. Polym. Sci. B **49**, 691 (2011).
[20] A. Arinstein, M. Burman, O. Gendelman, and E. Zussman, Nat. Nanotechnol. **2**, 59 (2007).
[21] O. Regev, R. Khalfin, E. Zussman, and Y. Cohen, Int. J. Biol. Macromol. **47**, 261 (2010).
[22] R. Carrotta, M. Manno, F. M. Giordano, A. Longo, G. Portale, V. Martorana, and P. L. S. Biagio, Phys. Chem. Chem. Phys. **11**, 4007 (2009).
[23] C. W. Macosko, *Rheology: Principles, Measurements, and Applications* (Wiley-VCH, New York, 1994).
[24] H. Qian, Protein Sci. **11**, 1 (2002).
[25] S. K. Jha and J. B. Udgaonkar, Proc. Natl. Acad. Sci. USA **106**, 12289 (2009).
[26] R. L. Baldwin, C. Frieden, and G. D. Rose, Proteins Struct. Funct. Bioinf. **78**, 2725 (2010).
[27] V. I. Goldanskii, M. A. Kozhushner, and L. I. Trakhtenberg, J. Phys. Chem. B **101**, 10024 (1997).
[28] U. W. Arndt and D. P. Riley, Philos. Trans. R. Soc. London A **247**, 409 (1955).
[29] F. R. Senti, M. J. Copley, and G. C. Nutting, J. Phys. Chem. **49**, 192 (1945).
[30] A. K. Rogozinsky and S. L. Bazhenov, Polymer **33**, 1391 (1992).